ЯДЕРНА ФІЗИКА
NUCLEAR PHYSICS

УДК 539.142 https://doi.org/10.15407/jnpae2024.01.026

A. H. Taqi*, W. A. Mansour

Department of Physics, College of Science, Kirkuk University, Kirkuk, Iraq

*Corresponding author: alitaqi@uokirkuk.edu.iq

ISOSCALAR GIANT QUADRUPOLE RESONANCE OF EVEN-EVEN $^{112\text{-}124}$Sn ISOTOPES USING BCS-QRPA

Using self-consistent Bardeen - Cooper - Schriffer + Hartree - Fock and quasiparticle random phase approximation, the isoscalar giant quadrupole resonance in the isotopes of ^{112,114,116,118,120,122,124}Sn has been studied in this work. Five sets of Skyrme-type interactions of different values of the nuclear matter incompressibility coefficient K_{NM} and effective mass m^*/m are used in the calculations. Additionally, the impact of different types of pairing forces (i.e., volume, surface, and mixed) is examined. Comparisons are made between the computed strength distributions, centroid energies E_{cen}, scaled energies E_s, and constrained energies E_{con} of the isoscalar giant quadrupole resonance and the available experimental data. Analysis is done on the relationships between K_{NM} and m^*/m, and the estimated properties.

Keywords: strength distribution, Skyrme force, Hartree - Fock + Bardeen - Cooper - Schrieffer, quasiparticle random phase approximation.

1. Introduction

Since our understanding of nuclear structure is still incomplete and unsatisfactory, theoretical and experimental studies were conducted to provide a method that could be used universally and accurately to explain nuclear structure. A many-body problem exists in the theoretical nuclear structure. It is impossible to compute the complete model space since the quantum many-body problem is a computational problem for which there is not yet a fully suitable answer. The self-consistent mean-field models is suitable to describe the nuclear structure [1, 2].

Inelastic electron and proton scattering research in the 1970s led to the discovery of the isoscalar giant quadrupole resonance (ISGQR) [3 - 5]. For an experimental review, we refer to [6]. Like the low-energy peak that appears in the isoscalar dipole response of neutron-rich nuclei [7], the low-lying quadrupole excitations rely on the number of particles outside closed shells [8]. The high-energy modes are expected to vary smoothly with the mass number A. In the case of the ISGQR, the excitation energy can be estimated to be proportional to the shell energy [9]. The comparison of microscopic self-consistent calculations with experiments on the ISGQR has provided valuable information on the value of effective mass m^* [10], one of the most important quantities that characterize nucleons embedded in the nuclear medium [11].

Microscopic models built on the self-consistent Hartree - Fock (HF) and Random Phase Approximation (RPA) are suitable for representing collective modes like ISGQR for closed-shell and closed sub-shell nuclei, where the HF theory has already been shown to be an effective method for describing the characteristics of ground states [12]. The result of nuclear pairing is essential in open-shell nuclei. HF + Bardeen - Cooper - Schriffer (HF+BCS) is a straightforward explanation for the ground-state pairing. Based on the HF+BCS model, the Quasiparticle Random Phase Approximation (QRPA) is an improved RPA model that takes into account the pairing effect, which is thought to be important for open-shell nuclei. This enables us to examine the entire nuclear chart's nuclear structure. Also, there are relativistic approaches like Relativistic Continuum Random Phase Approximation (RCRPA) [13] and Relativistic Quasi Particle Random Phase Approximation (RQRPA) [14].

Understanding the structure of nuclei and predicting the exotic properties of nuclei far from stability valley can both be done by studying the nuclear collective excitations. For modeling these collective excitations in open-shell nuclei with stable mean-field solutions, the QRPA is a widely used technique [15, 16]. The nuclear compressional modes, in particular the ISGQR, which provide the best method for determining nuclear incompressibility, are significant nuclear collective excitations [17, 18]. Nuclear collective excitations and nuclear incompressibility have lately been studied using both nonrelativistic RPA [19 - 22] and relativistic RPA or QRPA [13, 23].

Inelastic scattering of deuterons or alpha particles to modest forward angles is the main experimental technique for investigating the ISGQR. The methods created and put into use in the Research Center for

Nuclear Physics (RCNP) at Osaka University, Texas A&M University Cyclotron Institute, and Kernfysisch Versneller Instituut (KVI) in Groningen have made it possible to gather in-depth data on the ISGQR gross structure in a range of nuclear systems, see review [24].

In this study, the HF + Bardeen - Cooper - Schrieffer (HF+BCS) theory and the Skyrme QRPA method are used to explore the ISGQR of the Tin isotopes ^{112,114,116,118,120,122,124}Sn. The results are compared with the known experimental data [25 - 27]. The calculations used five different Skyrme parameter sets: T5 [28], SKM [29], SLY4 [30], SGII [31], and SKX [32]. The used Skyrme interactions exhibit a range of nuclear matter incompressibility $K_{\rm NM}$ and effective mass m^*/m. Additionally, we examine the effects of volume, surface, and mixed pairing interactions on the ISGQR characteristics of Sn isotopes.

2. Theoretical formulations

The nuclear properties of both ground states and excited states can be described by the Skyrme effective interaction (of parameters t_0, t_1, t_2, t_3, x_0, x_1, x_2, x_3, W_0 and α) [33 - 37]

$$V(r_1,r_2) = t_0(1+x_0\,P_\sigma)\delta(r_1-r_2)+\frac{t_1}{2}(1+x_1P_{12}^\alpha)\cdot\left[\overleftarrow{k}_{12}^2\delta(r_1-r_2)+\delta(r_1-r_2)\vec{k}_{12}^2\right]+$$

$$+\,t_2(1+x_2P_{12}^\alpha)\overleftarrow{k}_{12}\delta(r_1-r_2)\vec{k}_{12}+\frac{t_3}{6}(1+x_3P_{12}^\alpha)\rho^\alpha(R)\delta(r_1-r_2)+$$

$$+i\,W_0\overleftarrow{k}_{12}\delta(r_1-r_2)(\vec{\sigma}_1+\vec{\sigma}_2)\,\vec{k}_{12}, \qquad (1)$$

where $\vec{\sigma}_i$ is the Pauli spin operator, $\overleftarrow{k}_{12}=-\frac{i(\overleftarrow{\nabla}_1-\overleftarrow{\nabla}_2)}{2}$, $\vec{k}_{12}=-\frac{i(\vec{\nabla}_1-\vec{\nabla}_2)}{2}$, and P_{12}^α is the spin-exchange operator, the total energy E of HF equations based on Skyrme's interaction as a result of single-particle functions φ can be calculated using the variational approach $\delta\varphi|H(r)|\varphi=0$. The HF equations are coupled to the standard BCS equations, that in spherical symmetry the particle number n and gap equation Δ_a read as

$$n=\sum_a(2j_a+1)v_a^2, \quad \Delta_a=-\sum_b\frac{\Delta_b}{2E_b}V_{a\tilde{a}b\tilde{b}}, \qquad (2)$$

where the tilde designates the time-reversal state, and E and v are the typical quasi-particle energies and BCS amplitudes, respectively. The matrix elements $V_{a\tilde{a}b\tilde{b}}$ are calculated using a zero-range, density-dependent pairing force of the type,

$$V_{\rm pair}(\mathbf{r}_1,\mathbf{r}_2)=V_0\left[1+\eta\left(\frac{\rho\left(\frac{\mathbf{r}_1+\mathbf{r}_2}{2}\right)}{\rho_0}\right)\right]\delta(\mathbf{r}_1-\mathbf{r}_2), \qquad (3)$$

where the nuclear saturation density $\rho_0=0.16$ fm^{-1}. For the volume, mixed, or surface pairing interactions, the value of η is regarded as 0, 0.5, or 1, respectively. Table 1 contains the values of V_0 that we have determined by fitting the experimental data of the mean neutron gap of ^{120}Sn (Δ_n = 1.321 MeV). Due to the closed proton shells associated with Z = 50 in these nuclei, there is only neutron pairing.

Table 1. **Our obtained pairing strength V_0 to reproduce the empirical pairing gaps of ^{120}Sn (Δ_n = 1.321 MeV) for various types (volume, surface, and mixed) of pairing interactions defined in Eq. (3)**

Isotope	Skyrme-Type	Pairing strength V_0, MeV·fm^3		
		Volume	Surface	Mixed
^{112}Sn	T5	227	689	343
	SKM	231.5	741.5	355
	SLY4	269	792	404
	SGII	304	899	456
	SKX	200.5	731	315
^{114}Sn	T5	237.5	716	358
	SKM	226.5	728	347.5
	SLY4	272	799	407
	SGII	316.5	945	476
	SKX	201.3	733.5	317.5

Continuation of Table 1

Isotope	Skyrme-Type	Pairing strength V_0, MeV·fm^3		
		Volume	Surface	Mixed
^{116}Sn	T5	250	751.5	376.5
	SKM	224	725	344
	SLY4	277	815.5	414.5
	SGII	315.5	932.5	473.5
	SKX	201.5	738.5	317.5
^{118}Sn	T5	259.5	775.5	390.5
	SKM	225	733	345
	SLY4	282	832.5	423.5
	SGII	308.5	907.5	462
	SKX	200	736	316
^{120}Sn	T5	273	807	412
	SKM	228	750.5	351.5
	SLY4	286.5	855	430.5
	SGII	305	897	456
	SKX	203	750	320
^{122}Sn	T5	274.5	823	413.5
	SKM	234	782.5	362
	SLY4	290.5	874	438.5
	SGII	303.5	898	456
	SKX	207	770	328
^{124}Sn	T5	276	816	415
	SKM	245	830	381
	SLY4	298.5	908	451
	SGII	293	861.5	439.5
	SKX	215.4	809	340.8

The total HF+BCS energy can be calculated directly from the force or energy functional

$$E = E_{\mathrm{KE}} + E_{\mathrm{Skyrme}} + E_{\mathrm{Coul}} + E_{\mathrm{Pair}}, \qquad (4)$$

where E_{KE}, E_{Skyrme}, E_{Coul}, and E_{Pair} are the Kinetic, Skyrme, Coulomb, and Pair contributions to the energy, respectively.

First, a solution is found for the Skyrme HF+BCS equation for the ground state in coordinate space. The radial mesh used to solve the equations has a coverage area of up to 18 fm and a mesh size of 0.1 fm. This radial mesh is sufficiently large to generate stable results for all the nuclei under investigation.

To describe collective excitations in magic nuclei, the so-called RPA with stable mean-field solutions is typically used. The QRPA's expansion to open-shell nuclei comprises both the particle-particle and particle-hole channels. The Skyrme HF+BCS equations must be solved in order to acquire the ground state characteristics, which is the first step in solving the self-consistent QRPA. Based on the HF+BCS ground state, the ν-th excited state E_x^{ν} can be calculated within the QRPA model. The compact form of QRPA equations can be written as follows [38, 39]:

$$\begin{pmatrix} A_{ab,cd} & B_{ab,cd} \\ -B^*_{ab,cd} & -A^*_{ab,cd} \end{pmatrix} \begin{pmatrix} X^{\nu}_{cd} \\ Y^{\nu}_{cd} \end{pmatrix} = E^{\nu}_x \begin{pmatrix} X^{\nu}_{ab} \\ Y^{\nu}_{ab} \end{pmatrix}, \qquad (5)$$

where X^{ν} and Y^{ν} are the corresponding amplitudes. The matrices A and B on the HF+BCS two-quasiparticle bases have the form

$$A_{ab,cd} = \left(1+\delta_{ab}\right)^{-\frac{1}{2}} \left(1+\delta_{cd}\right)^{-\frac{1}{2}} \times$$

$$\times \Big[\left(E_a + E_b\right)\delta_{ac}\delta_{bd} + \left(u_a u_b u_c u_d + v_a v_b v_c v_d\right) G\left(abcd;J\right) + \left(u_a v_b u_c v_d + v_a u_b v_c u_d\right) F\left(abcd;J\right) -$$

$$-\left(-1\right)^{j_c + j_d - J'} \left(u_a v_b v_c u_d + v_a u_b u_c v_d\right) F\left(abdc;J\right) \Big], \qquad (6)$$

$$B_{ab,cd} = \left(1+\delta_{ab}\right)^{-\frac{1}{2}}\left(1+\delta_{cd}\right)^{-\frac{1}{2}} \times$$

$$\times\Big[-\left(u_a u_b v_c v_d + v_a v_b u_c u_d\right)G\left(abdc;J\right)-\left(-1\right)^{j_c+j_d-J'}\left(u_a v_b u_c v_d + v_a u_b v_c u_d\right)F\left(abcd;J\right)+$$

$$+\left(-1\right)^{j_a+j_b+j_c+j_d-J-J}\left(u_a v_b v_c u_d + v_a u_b u_c v_d\right)F\left(abcd;J\right)\Big] \quad (7)$$

with

$$G\left(abcd;J\right) =$$

$$= \sum_{m_a m_b m_c m_d} \left\langle j_a m_a j_b m_b \middle| JM\right\rangle \left\langle j_c m_c j_d m_d \middle| J'M'\right\rangle V^{pp}_{ab,cd}, \quad (8)$$

$$F\left(abcd;J\right) =$$

$$= \sum_{m_a m_b m_c m_d} \left\langle j_a m_a j_b m_b \middle| JM\right\rangle \left\langle j_c m_c j_d m_d \middle| J'M'\right\rangle V^{ph}_{ab,cd}. \quad (9)$$

$V^{pp}_{ab,cd}$ and $V^{ph}_{ab,cd}$ are matrix elements of particle-particle (pp) and particle-hole (ph) effective interaction, respectively. The ph matrix elements $V^{ph}_{ab,cd}$ is defined as [19]

$$V^{ph}_{ab,cd} = -\sum_{J'}\left(2J'+1\right)\begin{Bmatrix} j_a & j_d & J' \\ j_c & j_b & J \end{Bmatrix} V^{pp}_{ad,cb}. \quad (10)$$

The moments can be obtained using the following equation:

$$m_k = \int E^k S\left(E\right)dE, \quad (11)$$

where $S\left(E\right)$ is the strength function [17]

$$S\left(E\right) = \sum_{\nu}\left|\left\langle \nu\middle|\hat{F}_J\middle|0\right\rangle\right|^2 \rho_\Gamma\left(E-E_\nu\right) \quad (12)$$

associated with the monopole operator where the Lorentzian function is defined as in the following

$$\rho_\Gamma\left(E-E_\nu\right) = \frac{\Gamma}{2\pi}\frac{1}{\left(E-E_\nu\right)^2+\left(\frac{\Gamma}{2}\right)^2} \quad (13)$$

with Γ is the smearing parameter.

Three ratios can be calculated using these different sum rules: The centroid energy, $E_{\text{cen}} = m_1/m_0$, the constrained energy $E_{\text{con}} = \sqrt{m_1/m_{-1}}$, and the scaling energy $E_{\text{s}} = \sqrt{m_3/m_1}$, where m_1 is the energy-weighted sum rule (EWSR), m_{-1} is the inverse energy-weighted sum rule, and m_3 is the cubic energy-weighted sum rule [40].

3. Results and discussion

In Fig. 1, the calculated ISGQR strength distributions of ^{112,114,116,118,120,122,124}Sn isotopes are investigated by a modified version of the skyrme-rpa code [19] and compared with the available experimental data of Refs. [25, 26] (black error bars). The results were obtained with the five Skyrme sets: T5, SKM, SLY4, SGII, and SKX (the nuclear matter incompressibility coefficient K_{NM} and effective mass m^*/m of the studied Skyrme interactors are presented in Table 2) as a result of surface pairing, mixed pairing, and volume pairing forces (light green line, red line, and dark green line, respectively). We noted that surface pairing produces outcomes that are basically more in line with the experimental data. While the difference is fairly tiny, the peak energies predicted by the volume and mixed pairing are substantially lower.

The five Skyrme interactions result in a single peak roughly at 13 MeV. The link between interaction and peak energy is fundamentally different. The SKM and SLY4 results are in the center, followed by the SGII result, which is found at the maximum energy according to the corresponding incompressibility values, and SKX is remarkably similar to the experimental data. The T5 result is the lowest.

Table 3 displays the computed ISGQR centroid energy E_{cen}, restricted energy E_{con}, and scaling energy E_{s} for five sets of Skyrme parameters using the mixed pairing interaction. The experimental data was collected from Ref. [27]. The differences between theoretical values and experimental data are shown by the values in parentheses. The experimental data were overestimated by the SKM, SLY4, and SGII interactions while being underestimated by the T5 results. However, the SKX type is closer to the experimental data.

Fig. 2 depicts our calculated ISGQR centroid energy E_{cen}, constrained energy E_{con}, and scaling energy E_{s} with the experimental data [27] for the investigated Sn isotopes using different forces (T5, SKM, SLY4, SGII, and SKX) and pairing types (volume, surface, and mixed). The predicted

centroid energies generated by the SGII interaction do not match the experimental results. Furthermore, SKM and SLY4 predictions are noticeably more accurate. The SKX interaction, in contrast, closely resembles the experimental results, whereas the T5 results underestimated it even after pairing effects were considered.

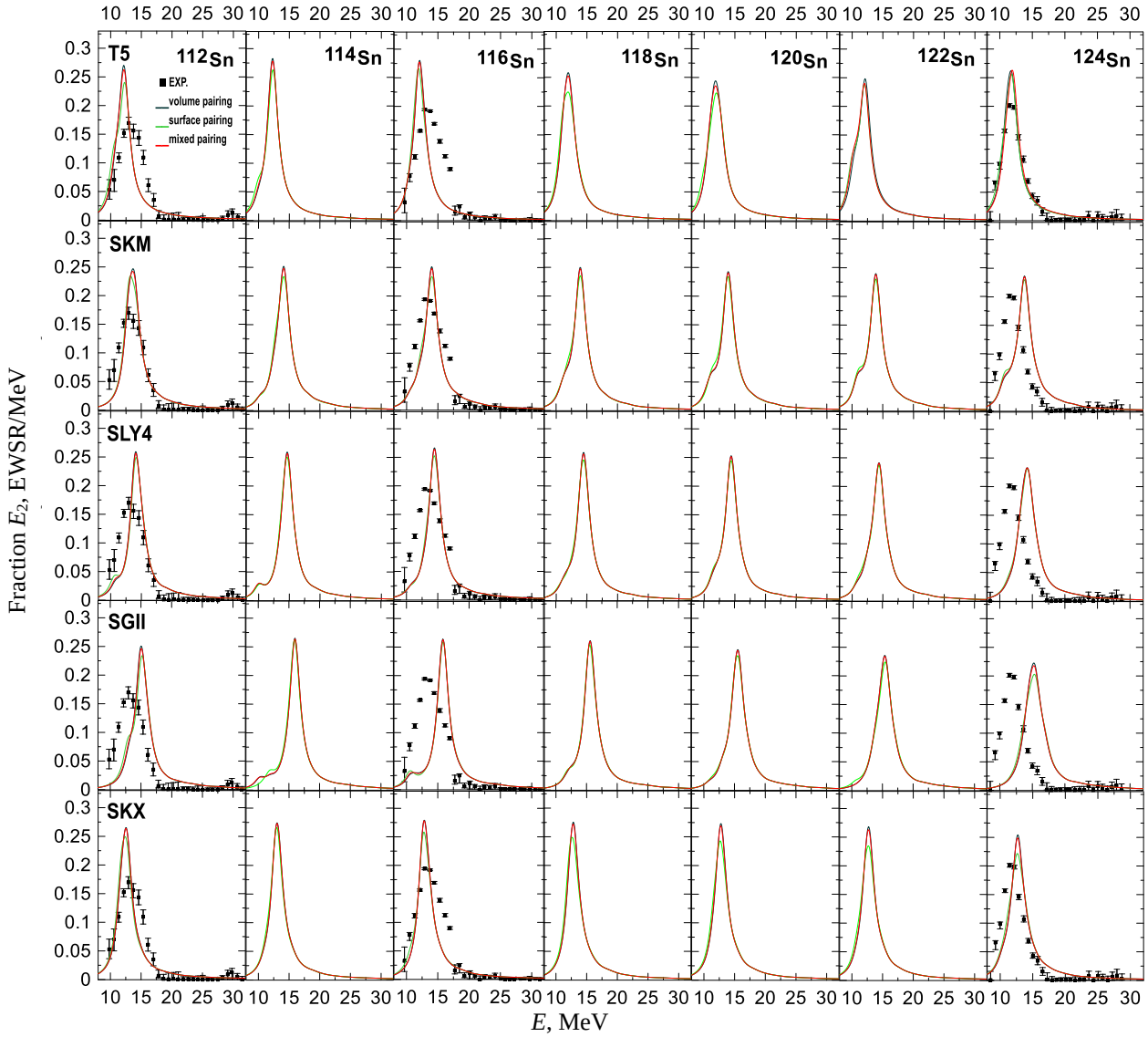

Fig. 1. The available experimental data [25, 26] for the examined Sn isotopes are compared with our calculated ISGQR strength distribution S (fm^4/MeV). The Skyrme forces T5, SKM, SLY4, SGII, and SKX are employed for the three different pairing types (volume, surface, and mixed). (See color Figure on the journal website.)

Table 2. **The nuclear matter incompressibility coefficient K_{NM} and effective mass m^*/m of the following Skyrme-type interaction**

Force	K_{NM}, MeV	m^*/m
T5	201.7	1
SKM	216.7	0.79
SLY4	229.9	0.69
SGII	269	0.79
SKX	270	0.99

With the exception of ^{112}Sn, the peak energies for the examined isotopes of Sn are better with the interaction SKX, which closely fits all of the energies defined in the text related to the experiment. The interaction T5 undervalues all of the energies defined in the text relative to the experiment, compared to SGII, which overvalues all of the energies.

As a result, there is still some mystery surrounding the difference between the values of the nuclear matter properties obtained from the Sn data. However, pairing effects must be taken into account to lessen the difference between the values of the nuclear matter properties extracted from Sn data.

Table 3. **The calculated E_{cen}, E_{con}, and E_s for ISGQR in the investigated Sn isotopes by combining the mixed pairing interaction with the parameter sets for T5, SKM, SLY4, SGII, and SKX**

Isotope	Exp.	T5	SKM	SLY4	SGII	SKX
	E_{cen}, MeV					
^{112}Sn	13.4 ± 0.1	12.08 (1.32)	13.66 (–0.26)	14.01 (–0.61)	14.98 (–1.58)	12.60 (0.8)
^{114}Sn	13.2 ± 0.1	12.21 (0.99)	13.90 (–0.7)	14.34 (–1.14)	15.66 (–2.46)	13.14 (0.06)
^{116}Sn	13.1 ± 0.1	12.12 (0.98)	13.79 (–0.69)	14.36 (–1.26)	15.33 (–2.23)	13.06 (0.04)
^{118}Sn	13.1 ± 0.1	12.00 (1.1)	13.69 (–0.59)	14.24 (–1.14)	15.45 (–2.35)	12.98 (0.12)
^{120}Sn	12.9 ± 0.1	11.91 (0.99)	13.60 (–0.7)	14.17 (–1.27)	15.36 (–2.46)	12.90 (0)
^{122}Sn	12.8 ± 0.1	11.82 (0.98)	13.49 (–0.69)	14.11 (–1.31)	15.26 (–2.46)	12.81 (–0.01)
^{124}Sn	12.6 ± 0.1	11.88 (0.72)	13.42 (–0.82)	14.15 (–1.55)	15.26 (–2.66)	12.70 (–0.1)
	E_{con}, MeV					
^{112}Sn	13.4 ± 0.1	12.03 (1.37)	13.61 (–0.21)	13.89 (–0.49)	14.89 (–1.49)	12.56 (0.84)
^{114}Sn	13.2 ± 0.1	12.16 (1.04)	13.81 (–0.61)	14.23 (–1.03)	15.55 (–2.35)	13.10 (0.1)
^{116}Sn	13.1 ± 0.1	12.08 (1.02)	13.71 (–0.61)	14.28 (–1.18)	15.15 (–2.05)	13.03 (0.07)
^{118}Sn	13.1 ± 0.1	11.96 (1.14)	13.61 (–0.51)	14.16 (–1.06)	15.37 (–2.27)	12.94 (0.16)
^{120}Sn	12.9 ± 0.1	11.87 (1.03)	13.52 (–0.62)	14.09 (–1.19)	15.27 (–2.37)	12.86 (0.04)
^{122}Sn	12.8 ± 0.1	11.75 (1.05)	13.39 (–0.59)	14.02 (–1.22)	15.16 (–2.36)	12.78 (0.02)
^{124}Sn	12.6 ± 0.1	11.84 (0.76)	13.31 (–0.71)	14.08 (–1.48)	15.18 (–2.58)	12.64 (–0.04)
	E_s, MeV					
^{112}Sn	13.4 ± 0.1	12.49 (0.91)	14.10 (–0.7)	14.53 (–1.13)	15.52 (–2.12)	13.11 (0.29)
^{114}Sn	13.2 ± 0.1	12.44 (0.76)	14.20 (–1)	14.71 (–1.51)	16.03 (–2.83)	13.23 (–0.03)
^{116}Sn	13.1 ± 0.1	12.34 (0.76)	14.10 (–1)	14.63 (–1.53)	15.85 (–2.75)	13.14 (–0.04)
^{118}Sn	13.1 ± 0.1	12.23 (0.87)	14.01 (–0.91)	14.54 (–1.44)	15.78 (–2.68)	13.07 (0.03)
^{120}Sn	12.9 ± 0.1	12.16 (0.74)	13.94 (–1.04)	14.47 (–1.57)	15.70 (–2.8)	12.99 (–0.09)
^{122}Sn	12.8 ± 0.1	12.10 (0.7)	13.87 (–1.07)	14.43 (–1.63)	15.62 (–2.82)	12.92 (–0.12)
^{124}Sn	12.6 ± 0.1	12.13 (0.47)	13.81 (–1.21)	14.44 (–1.84)	15.61 (–3.01)	12.87 (–0.27)

N o t e. The experimental information was collected from Ref. [27]. The difference between theoretical values and experimental data is shown by the quantities in parentheses.

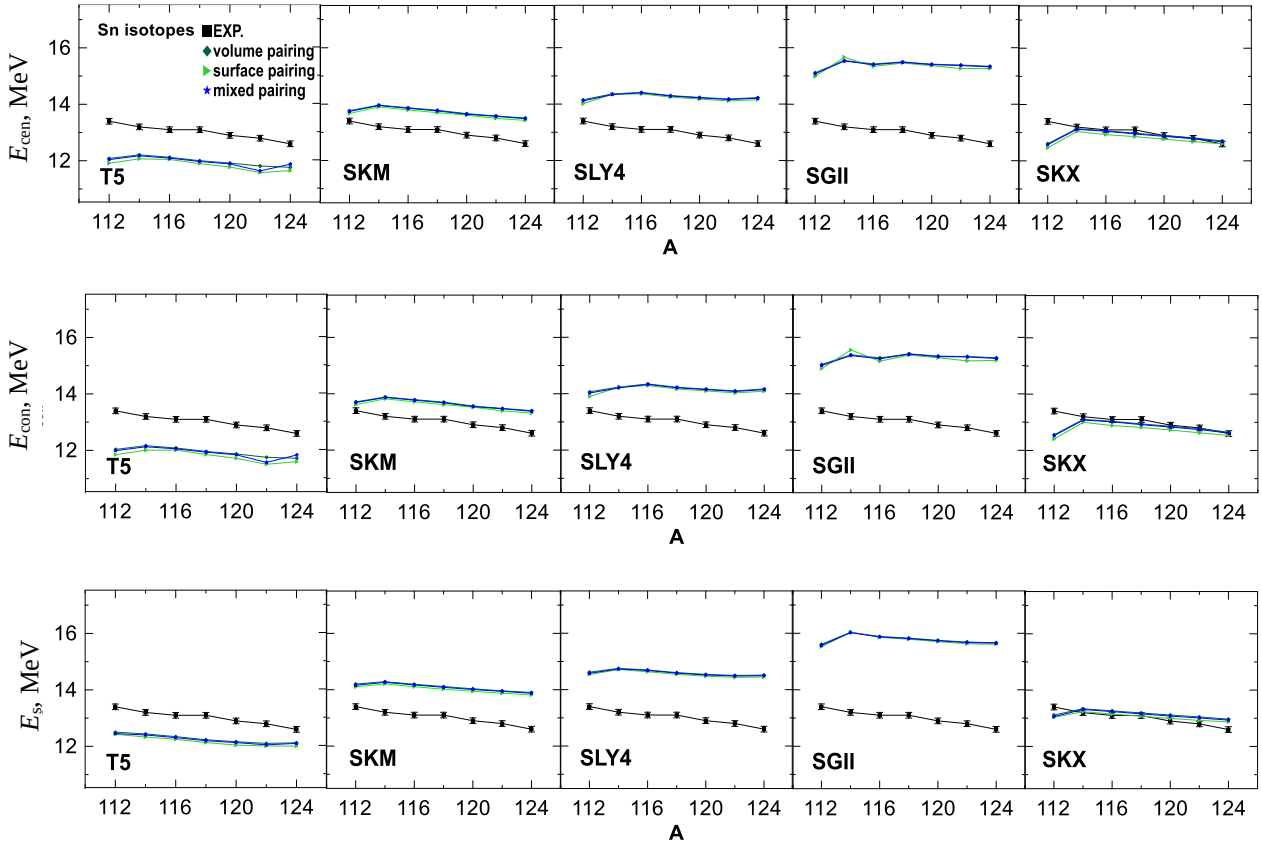

Fig. 2. Our calculated ISGQR centroid energy E_{cen}, constrained energy E_{con}, and scaling energy E_s are compared with the experimental data [27] for the investigated Sn isotopes. Different pairing types (volume, surface, and mixed) are applied using the forces T5, SKM, SLY4, SGII, and SKX. (See color Figure on the journal website.)

Figs. 3 and 4 illustrate the calculated and measured data [27] of ISGQR centroid energy E_{cen}, constrained energy E_{con}, and scaling energy E_s versus nuclear incompressibility constant K_{NM} and effective mass m^*/m, respectively for the investigated ^{112,114,116,118,120,122,124}Sn isotopes. The forces T5, SKM, SLY4, SGII, and SKX are adopted along K_{NM} and m^*/m for various types of pairing (volume, surface, and mixed).

It is clear from Fig. 3 that there is a strong correlation between the calculated energies (E_{cen}, E_{con}, and E_s) and the nuclear incompressibility constant K_{NM}, but there is an effect of the effective mass m^*/m as shown in Fig. 4.

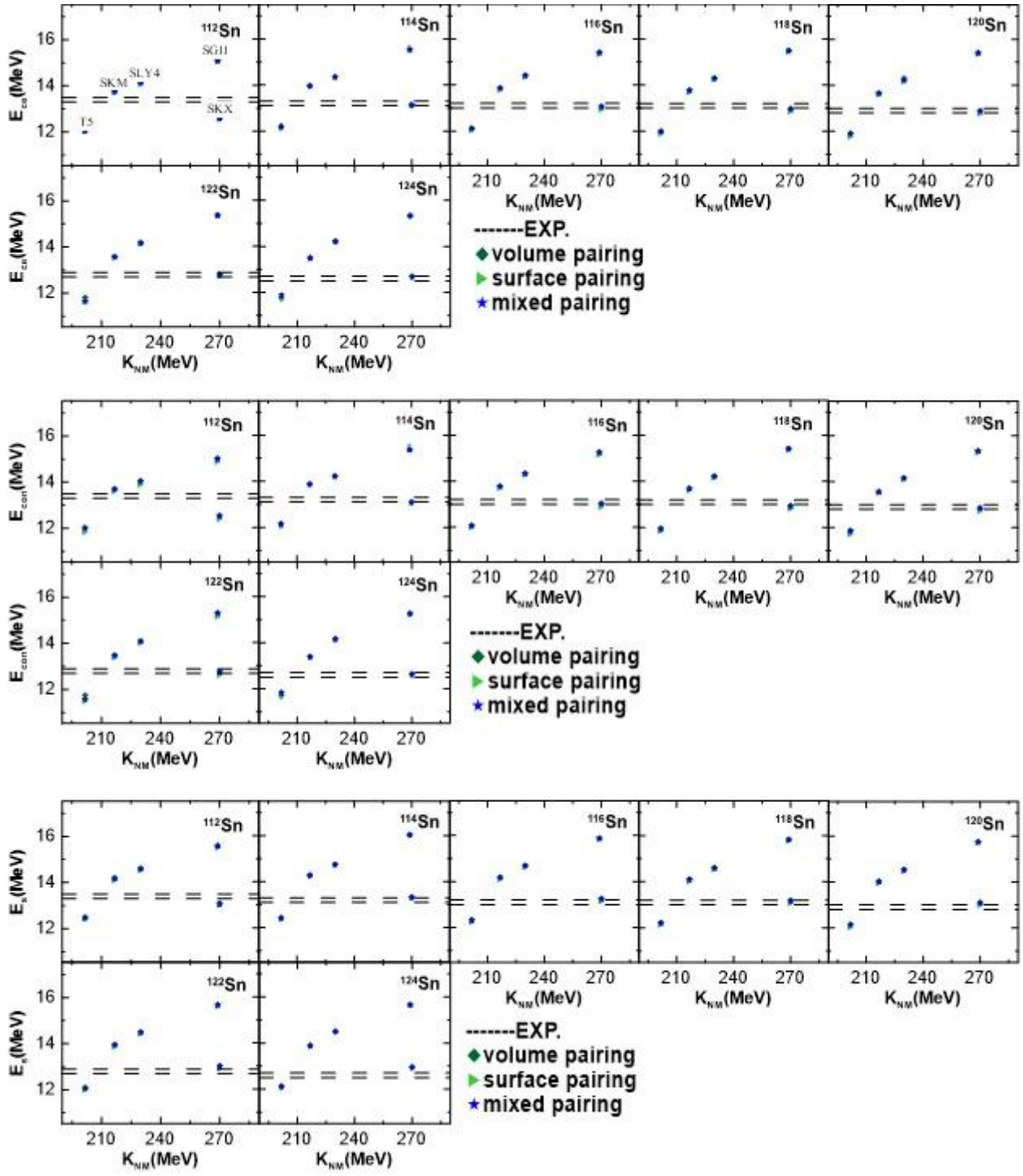

Fig. 3. The calculated ISGQR centroid energy E_{cen}, constrained energy E_{con}, and scaling energy E_s versus nuclear incompressibility constant K_{NM} are compared with the experimental data [27] for the investigated Sn isotopes. The forces T5, SKM, SLY4, SGII, and SKX are adopted along K_{NM} for various types of pairing (volume, surface, and mixed). (See color Figure on the journal website.)

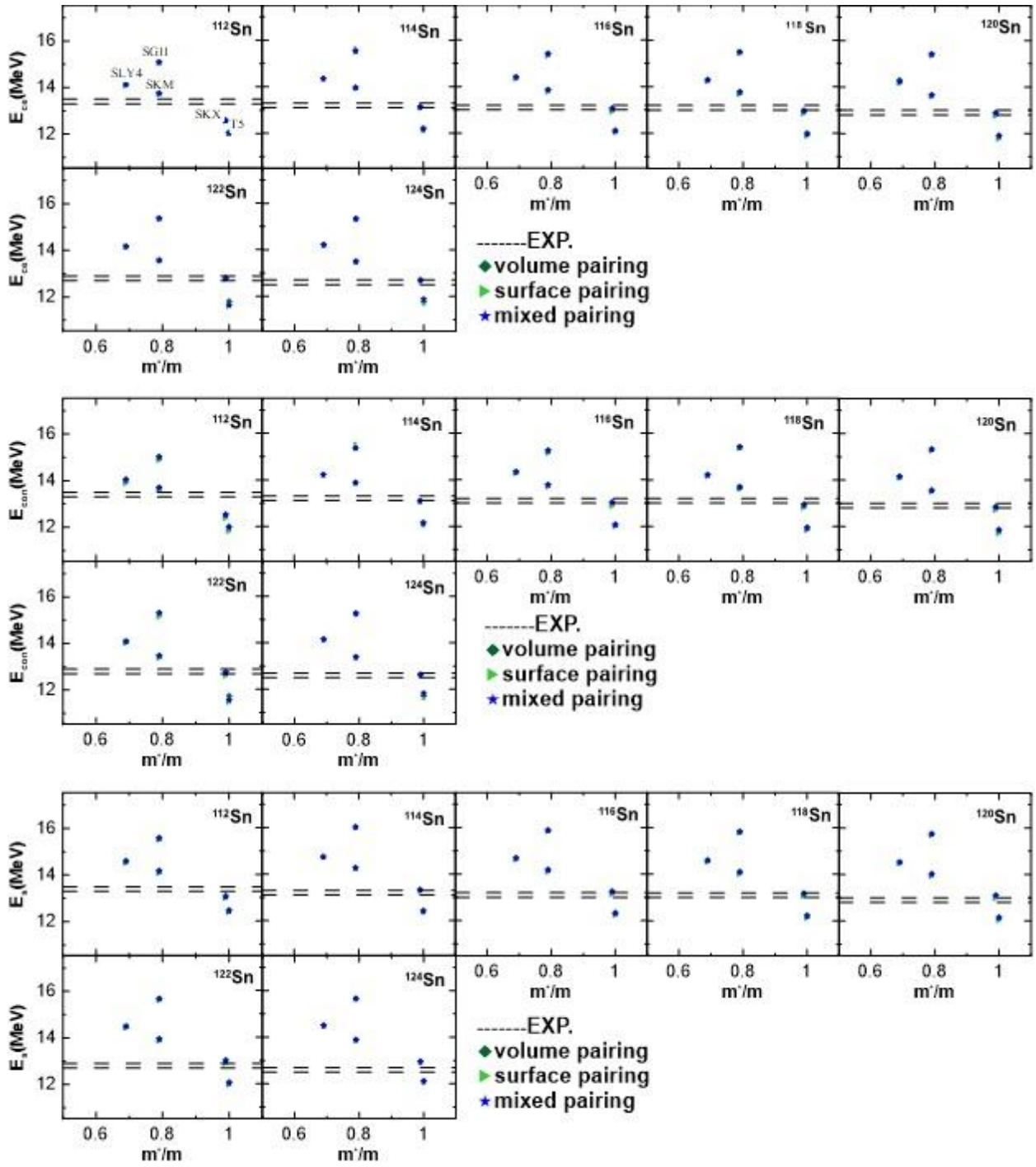

Fig. 4. The calculated ISGQR centroid energy E_{cen}, constrained energy E_{con}, and scaling energy E_{s} versus nuclear matter effective mass m^*/m are compared with the experimental data [27] for the investigated Sn isotopes. The forces T5, SKM, SLY4, SGII, and SKX are adopted along K_{NM} for various types of pairing (volume, surface, and mixed). (See color Figure on the journal website.)

Our results using the T5 and SKX types were lower than the experimental data, these types have high m^*/m values close to 1 and 0.99, respectively, noting that the T5 type has the lowest value of $K_{\text{MN}} = 201.7$ MeV and the SKX type has the highest value $K_{\text{MN}} = 270$ MeV. While results using the SKM, SLY4, and SGII types were higher than the experimental data, these types have K_{MN} values 216.7, 229, and 269 MeV, respectively, noting that the SLY4 type has $m^*/m = 0.69$ and the types SKM and SGII have the same effective mass $m^*/m = 0.79$.

4. Conclusions

The ISGQR in even-even $^{112\text{-}124}$Sn isotopes is investigated using self-consistent Skyrme HF + BCS, and QRPA. The calculations in this work make use of five different Skyrme parameter sets: T5, SKM, SLY4, SGII, and SKX; they were picked because

they have various values of nuclear incompressibility K_{NM} and effective mass m^*/m. Three pairing interactions the so-called volume, surface, and mixed pairing forces are the ones we pick to examine the function of pairing correlations. The available experimental data are compared to the scaling energy E_s, restricted energy E_{con}, and centroid energy E_{cen} of the ISGQR. The current investigation reveals a strong correlation between the calculated energies (E_{cen}, E_{con}, and E_s) and the nuclear incompressibility constant K_{NM}, but there is an effect of the effective mass m^*/m. The Skyrme-types T5 and SKX of m^*/m values 1 and 0.99 and K_{MN} values 201.7 and 270 MeV, respectively have significantly underestimated the data. While results using the SKM, SLY4, and SGII of K_{MN} values 216.7, 229, and 269 MeV, respectively, noting that the SLY4 type has $m^*/m = 0.69$ and the types SKM and SGII have the same effective mass $m^*/m = 0.79$. A better description of the ISGQR is obtained by using the force SKX parameter (with associated incompressibility of $K_{MN} = 270$ MeV and $m^*/m = 0.99$) is closer to the experimental data. As well as we concluded that the gap between the nuclear incompressibility values obtained from the Sn data is reduced with the use of pairing, and the surface pairing generates results that are essentially closer to the experimental data.

REFERENCES

1. P. Ring, P. Schuck. *The Nuclear Many-Body Problem*. 1st ed. (New York, Berlin, Springer-Verlag, 1980) 716 p.
2. J.-P. Blaizot, G. Ripka. *Quantum Theory of Finite Systems* (MIT Press Cambridge, 1986) 657 p.
3. R. Pitthan, T. Walcher. Inelastic electron scattering in the giant resonance region of La, Ce and Pr. Phys. Lett. B 36 (1971) 563.
4. S. Fukuda, Y. Torizuka. Giant Multipole Resonances in ^{90}Zr Observed by Inelastic Electron Scattering. Phys. Rev. Lett. 29 (1972) 1109.
5. M. Lewis, F. Bertrand. Evidence from inelastic proton scattering for a giant quadrupole vibration in spherical nuclei. Nucl. Phys. A 196 (1972) 337.
6. M.N. Harakeh, A. van der Woude. *Giant Resonances: Fundamental High-Frequency Modes of Nuclear Excitation* (Oxford University Press, 2001) 638 p.
7. N. Tsoneva, H. Lenske. Pygmy Quadrupole Resonance in skin nuclei. Phys. Lett. B 695 (2011) 174.
8. X. Roca-Maza et al. Low-lying dipole response: Isospin character and collectivity in ^{68}Ni, ^{132}Sn, and ^{208}Pb. Phys. Rev. C 85 (2012) 024601.
9. A. Bohr, B.R. Mottelson. *Nuclear Structure.* Vol. I: *Single-Particle Motion*; Vol. II: *Nuclear Deformations* (New York, Amsterdam: W. A. Benjamin, Inc., 1975).
10. J.P. Blaizot. Nuclear compressibilities. Phys. Rep. 64 (1980) 171.
11. C. Mahaux et al. Dynamics of the shell model. Phys. Rep. 120 (1985) 1.
12. N.V. Giai. Self-Consistent Description of Nuclear Excitations. Prog. Theor. Phys. Supp. 74-75 (1983) 330.
13. D. Vretenar, T. Nikšić, P. Ring. A microscopic estimate of the nuclear matter compressibility and symmetry energy in relativistic mean-field models. Phys. Rev. C 68 (2003) 024310.
14. I. Daoutidis. Relativistic Continuum Random Phase Approximation in Spherical Nuclei. PhD thesis (Technical University of Munich, 2009).
15. A.H. Taqi, G.A. Mohammed. Isoscalar monopole response in the neutron-rich molybdenum isotopes using self-consistent QRPA. Nucl. Phys. At. Energy 24 (2023) 306.
16. D.J. Rowe. *Nuclear Collective Motion: Models and Theory* (London, Methuen, 1970) 340 p.
17. G. Colò et al. Microscopic determination of the nuclear incompressibility within the nonrelativistic framework. Phys. Rev. C 70 (2004) 024307.
18. S. Shlomo, V.M. Kolomietz, G. Colò. Deducing the nuclear-matter incompressibility coefficient from data on isoscalar compression modes. Eur. Phys. J. A 30 (2006) 23.
19. G. Colò et al. Self-consistent RPA calculations with Skyrme-type interactions: The skyrme_rpa program. Comp. Phys. Comm. 184 (2013) 142.
20. S. Péru, J.F. Berger, P.F. Bortignon. Giant resonances in exotic spherical nuclei within the RPA approach with the Gogny force. Eur. Phys. J. A 26 (2005) 25.
21. T. Sil et al. Effects of self-consistency violation in Hartree-Fock RPA calculations for nuclear giant resonances revisited. Phys. Rev. C 73 (2006) 034316.
22. H. Sagawa et al. Isospin dependence of incompressibility in relativistic and nonrelativistic mean field calculations. Phys. Rev. C 76 (2007) 034327.
23. J. Piekarewicz. Why is the equation of state for tin so soft? Phys. Rev. C 76 (2007) 031301(R).
24. U. Garg, G. Colò. The compression-mode giant resonances and nuclear incompressibility. Prog. Part. Nucl. Phys. 101 (2018) 55.
25. Y.-W. Lui et al. Giant resonances in ^{112}Sn and ^{124}Sn: Isotopic dependence of monopole resonance energies. Phys. Rev. C 70 (2004) 014307.
26. D.H. Youngblood et al. Isoscalar E0 - E3 strength in ^{116}Sn, ^{144}Sm, ^{154}Sm, and ^{208}Pb. Phys. Rev. C 69 (2004) 034315.
27. T. Li et al. Isoscalar giant resonances in the Sn nuclei and implications for the asymmetry term in the nuclear-matter incompressibility. Phys. Rev. C 81 (2010) 034309.
28. F. Tondeur et al. Static nuclear properties and the parametrisation of Skyrme forces. Nucl. Phys. A 420 (1984) 297.
29. A.M. Saruis. Self-consistent HF-RPA description of electron and photon nuclear reactions with Skyrme forces. Phys. Rep. 235 (1993) 57.
30. J. Rikovska Stone et al. Nuclear matter and neutron-star properties calculated with the Skyrme interaction. Phys. Rev. C 68 (2003) 034324.

31. N. Van Giai, H. Sagawa. Spin-isospin and pairing properties of modified Skyrme interactions. Phys. Lett. B 106 (1981) 379.
32. B.A. Brown. New Skyrme interaction for normal and exotic nuclei. Phys. Rev. C 58 (1998) 220.
33. J.R. Stone, P.-G. Reinhard. The Skyrme interaction in finite nuclei and nuclear matter. Prog. Part. Nucl. Phys. 58 (2007) 587.
34. A.H. Taqi, G.L. Alawi. Isoscalar giant resonance in ^{100,116,132}Sn isotopes using Skyrme HF-RPA. Nucl. Phys. A 983 (2019) 103.
35. A.H. Taqi, M.S. Ali. Self-consistent Hartree-Fock RPA calculations in ^{208}Pb. Indian J. Phys. 92 (2017) 69.
36. A.H. Taqi, E.G. Khidher. Ground and transition properties of ^{40}Ca and ^{48}Ca nuclei. Nucl. Phys. At. Energy 19 (2018) 326.
37. Sh.H. Amin, A.A. Al-Rubaiee, A.H. Taqi. Effect of Incompressibility and Symmetry Energy Density on Charge Distribution and Radii of Closed-Shell Nuclei. Kirkuk Journal of Science 17 (2022) 17.
38. J. Kvasil et al. Deformation-induced splitting of the isoscalar E0 giant resonance: Skyrme random-phase-approximation analysis. Phys. Rev. C 94 (2016) 064302.
39. K. Yoshida, T. Nakatsukasa. Shape evolution of giant resonances in Nd and Sm isotopes. Phys. Rev. C 88 (2013) 034309.
40. S. Stringari. Sum rules for compression modes. Phys. Lett. B 108 (1982) 232.

А. Х. Такі*, В. А. Мансур

Кафедра фізики, Освітній коледж, Університет Кіркука, Кіркук, Ірак

*Відповідальний автор: alitaqi@uokirkuk.edu.iq

ІЗОСКАЛЯРНИЙ ГІГАНТСЬКИЙ КВАДРУПОЛЬНИЙ РЕЗОНАНС ПАРНО-ПАРНИХ ІЗОТОПІВ $^{112\text{-}124}$Sn З ВИКОРИСТАННЯМ МЕТОДУ BCS-QRPA

У цій роботі було вивчено ізоскалярний гігантський квадрупольний резонанс ізотопів ^{112,114,116,118,120,122,124}Sn із застосуванням самоузгодженого методу Бардіна - Купера - Шріффера + Хартрі - Фока та квазічастинкового наближення випадкових фаз. У розрахунках використано п’ять наборів взаємодій типу Скірма з різними значеннями коефіцієнта нестисливості ядерної речовини K_{NM} та ефективної маси m^*/m. Крім того, досліджується вплив різних типів сил спарювання (об’ємних, поверхневих і змішаних). Проведено порівняння між обчисленими силовими розподілами, енергіями центроїда E_{cen}, масштабованими енергіями E_s і обмежувальними енергіями E_{con} ізоскалярного гігантського квадрупольного резонансу та доступними експериментальними даними. Проведено аналіз зв’язків між K_{NM} і m^*/m з оціненими властивостями.

Ключові слова: силовий розподіл, сили Скірма, Хартрі - Фок + Бардін - Купер - Шріффер, квазічастинкове наближення випадкових фаз.

Надійшла/Received 27.09.2023